Int. J. Electrochem. Sci., 15 **(2020)** 12030 – 12040, doi: 10.20964/2020.12.41

International Journal of
ELECTROCHEMICAL
SCIENCE
www.electrochemsci.org

A study of $La_{1-x}Sr_xCoO_{3-\delta}$ SOFC Cathodes using Cone-shaped Electrodes and EIS

K. Kammer Hansen

Kammer Consulting, Skelbækparken 91, DK-3650 Ølstykke, Denmark
E-mail: kkha@dtu.dk

Received: 17 August 2020 / *Accepted:* 2 October 2020 / *Published:* 31 October 2020

Six strontium substituted lanthanum cobaltite's ($La_{1-x}Sr_xCoO_{3-\delta}$, x=0, 0.05, 0.15, 0.25, 0.35 and 0.5) were synthesized using the glycine-nitrate process. The cobaltites were characterized with powder XRD, dilatometry, 4-point DC conductivity measurements and electrochemical impedance spectroscopy on cone-shaped electrodes using a $Ce_{1.9}Gd_{0.1}O_{1.95}$ electrolyte. All the compounds were single phased belonging to hexagonal crystal system. The thermal expansion coefficient decreases until a strontium content of 15% where after it increases. The conductivity increased for temperatures below 600 ^oC with increasing strontium content. At higher temperatures the conductivity increased until the strontium content reached 15%, where after it began to decrease. It was shown that the activity of the cobaltite's were strongly dependent on the strontium content. The highest activity, towards the reduction of oxygen, was found for the strontium rich composition, $La_{0.5}Sr_{0.5}CoO_{3-\delta}$, with an area specific resistance of 0.92 Ωcm^2 at 600^{o}C. It was concluded that the activity of the cobaltites towards the reduction of oxygen is determined mainly by the oxide ionic conductivity.

Keyword: SOFC; Cobaltite's; Oxygen reduction; Cones

1. INTRODUCTION

The solid oxide fuel cell (SOFC) converts chemical energy directly in to heat and electricity in a simple and (cost) efficient manner [1]. However, in order to commercialize the SOFC a decrease of the operation temperature is needed, as this will lead to a necessary lowering of the cost [2]. Several improvements have already been done, and the operating temperature has at present been lowered to around 650 ^oC [3]. Improvement of the electrodes is one way to further lower the operating temperature. The classical SOFC cathode strontium substituted lanthanum manganite (LSM) and yttria stabilized zirconia (YSZ) composite electrode do not have a enough activity at temperatures, at these intermediate temperatures [4]. Alternatives are Fe, Fe-Co or Co based perovskite oxide materials, see [5]. Among them Co based perovskite oxides are normally considered to be the most efficient alternative [6].

LSCox ($La_{1-x}Sr_xCoO_{3-\delta}$) based perovskite oxides are characterized with a high electronic and ionic conductivity, a high thermal expansion coefficient and chemical instability towards the commonly used electrolyte YSZ [7]. Whereas the first two properties are highly appreciated, the last two complicates the use of the cobaltite's as cathodes in a SOFC. In order to solve this, the LSCo's are mixed with the electrolyte and a barrier layer is added between the cathode and the electrolyte.

The defect chemistry of LSCo perovskites has been treated in detail in the literature [8]. The defect chemistry of LSCo perovskites cannot be described satisfactory using a simple point defect model. Instead another model has been suggested. In this model it is assumed that cobalt 3d-orbitals and oxygen 2p-orbitals form a conduction band.

The oxygen non-stoichiometry of LSCo perovskites has been investigated in the literature [10]. It has been shown that the oxygen non-stoichiometry increases with increasing strontium content. Also the oxygen non-stoichiometry is temperature dependent, it increases with increasing temperature. Is has been shown that the ionic conductivity of cobalt based perovskites increases with increasing strontium content [10].

In this work strontium substituted lanthanum cobaltite's are synthesized using the glycine-nitrate process [11] and studied using cone-shaped electrodes in combination with electrochemical impedance spectroscopy (EIS) as cathodes in a SOFC. In addition to this the perovskite oxides are evaluated by powder XRD, dilatometry and 4-point DC-conductivity measurements.

Model electrodes are to a large extent used in the literature to study SOFC electrodes [12]. The most used technique is thin film electrodes [13]. However, the use of cone-shaped electrodes is a simple and convenient alternative. It was first suggested by Fabry and Kleitz [14]. There are several reasons for why it is useful to take advantage of the cone-shaped electrode technique. As the cone and the electrolyte are sintered separately, there is no reaction between these during processing. Furthermore, as the electrode material not is mixed with electrolyte powder the true electro-catalytic properties of the electrode is less itinerated than by using porous composite electrodes. In addition to this the contact areas of the cone-shaped electrodes can be found from Newman's formula (1), as the contact area in principle has a simple circular geometry [15]:

$$r = \frac{1}{4R_s\sigma^*}, \quad (1)$$

where R_s is the series resistance and σ^* is the specific conductivity of the ceria based electrolyte. As electrolyte resistance a value of 0.0167 scm^{-1} at 600 ^oC was used throughout [16]. The cone-shaped electrode set-up used in this study is a pseudo three-electrode set-up as the counter/reference electrode is much larger in area than the cone-shaped electrode, see figure 1.

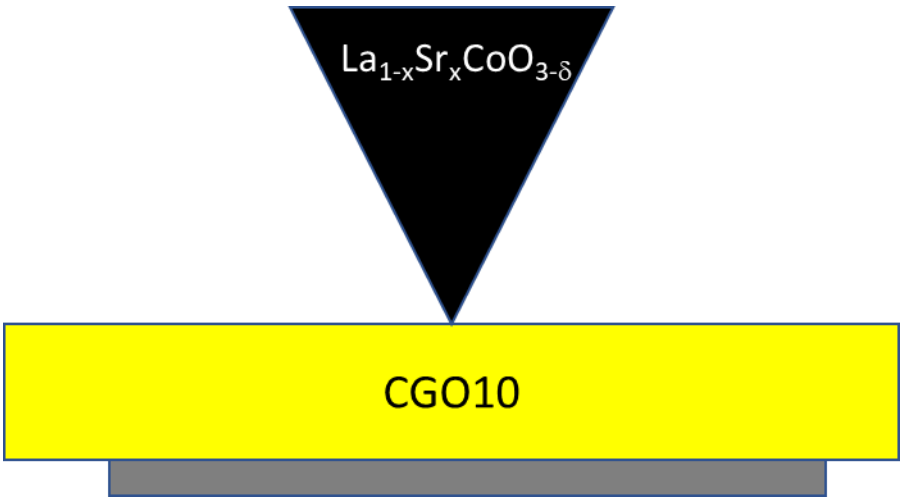

Figure 1. Schematic drawing of the experimental set-up. The cone-shaped electrode is pressed towards the electrolyte with a small weight (not shown). The set-up is a three electrode set-up, as the cone-shaped electrode is much smaller in size than the counter/working electrode (bottom).

We have before been using cone-shaped electrode for comparable studies of different compositions of electrode materials [17]. For this the cone-shaped electrode technique is very useful.

The literature on cobaltite's as SOFC cathodes is very comprehensive, but to the authors knowledge no study, where the composition is varied systematically is present in the open literature. Here, I for the first time present such a study.

The results obtained in this study are discussed in the light of a mechanism suggested in the literature for mixed ionic and electronic conductors [18] and compared with my two previous papers on LSM and strontium substituted lanthanum ferrites (LSF) [19, 20].

2. EXPERIMENTAL

The cobaltites were prepared using the glycine-nitrate route [11]. In short, the metal nitrates dissolved in water were mixed in the appropriate ratio in a beaker. Glycine was then added. After this the mixture was heated on a hot plate until ignition. The resulting powders were then transferred to alumina crucibles and calcined at 1000^{o}C for 6 hours in air in a box furnace. The phase purity was checked using a Stoe theta-theta diffractometer equipped with $Cu_{k\alpha}$ radiation. The powders were pressed into bars and cylinders using appropriate dies. The bars and cylinders were then sintered at 1250^{o}C/12 h in air in a box furnace. After this the cylinders were machined into cone-shaped electrodes. The cone-shaped electrodes had a base of 7.5 mm and sides with an angle of 45^{o}. Dilatometry was recorded using a Netsch 402CD dilatometer. The heating and cooling rate was 100^{o}C/h. Two hours rest at 1000^{o}C. 4-point DC conductivity data were measured and collected with a PC-Keithley micro ohmmeter set-up and in-house software to collect the conductivity data and control the temperature. The heating and cooling ramps were 3^{o}C/min. The samples were heated in increments of 50 ^{o}C. The samples were kept at temperature for two hours. Conductivity measurements were performed every fifth minute.

For the electrochemical measurements a set-up, as illustrated in figure 1, with a CGO10 electrolyte pellets was used. The electrolyte pellets were prepared by pressing CGO10 powder (Rhodia) in a die followed by sintering at 1500ºC/2h in air in a box furnace. The pellets were polished on one side with diamond paste to 1 μm. As a counter/reference electrode Pt-paste (Engelhard) was added and sintered in-situ at 800ºC. The EIS data were recorded using a Gamry reference 600 potentiostat. The EIS were recorded in the frequency range 1 MHz to 0.05 Hz with 6 points recorded at each decade. As amplitude 24 mV root mean square (rms) was used throughout. The measurements were done in air. The fitting of the EIS data were done using the PC-DOS program 'equivcrt' [21]. At first the data were fitted with all values set free. Then the average of the n-values was taken and the fit was repeated again with constant n.

3. RESULTS

The results from the powder diffraction can be found in Table 1. The Rietveld refinements were done using the software Winpow (DTU Chemistry, Denmark). All the powders are found to be phase pure and belong to the hexagonal crystal system. The a-axis decreases with increasing strontium content, whereas the c-axis decreases with increasing strontium content.

The thermal expansion coefficient (TEC) for the investigated Cobaltite's can be found in table 2. The behavior is not straight forward, as the intermediate compound LSCo15 has the lowest thermal expansion coefficient. The values are relatively high and reached its maximum for the strontium rich compound LSCo50 with a value as high as $25.7*10^{-6}$ K^{-1}.

Table 1. The powder XRD data after Rietveld refinements. The a-axis decreases, whereas the c-axis increases with increasing strontium content. This is an indication of the Jahn-Teller effect. Units in Å.

La_{1-x} $Sr_xCoO_{3-\delta}$. Crystal structure R-3c							
Material	**Sr %**	**a**	**Error**	**c**	**Error**	**Volume**	**Error**
LaCo	0	5.448	0.001	13.107	0.001	336.93	0.03
LaCoSr5	5	5.449	0.001	13.125	0.001	337.46	0.03
LaCoSr15	15	5.447	0.001	13.159	0.001	338.13	0.02
LaCoSr25	25	5.445	0.001	13.194	0.001	338.83	0.03
LaCoSr35	35	5.437	0.001	13.211	0.002	338.23	0.04
LaCoSr50	50	5.425	0.001	13.235	0.002	337.12	0.11

Table 2. The thermal expansion coefficient (TEC) of the cobaltite's. The TEC finds its maximum for the strontium rich compound LSCo50. Unit in 10^{-6} K^{-1}.

X	0	5	15	25	35	50
TEC	22.89	21.71	19.71	20.10	24.57	25.69

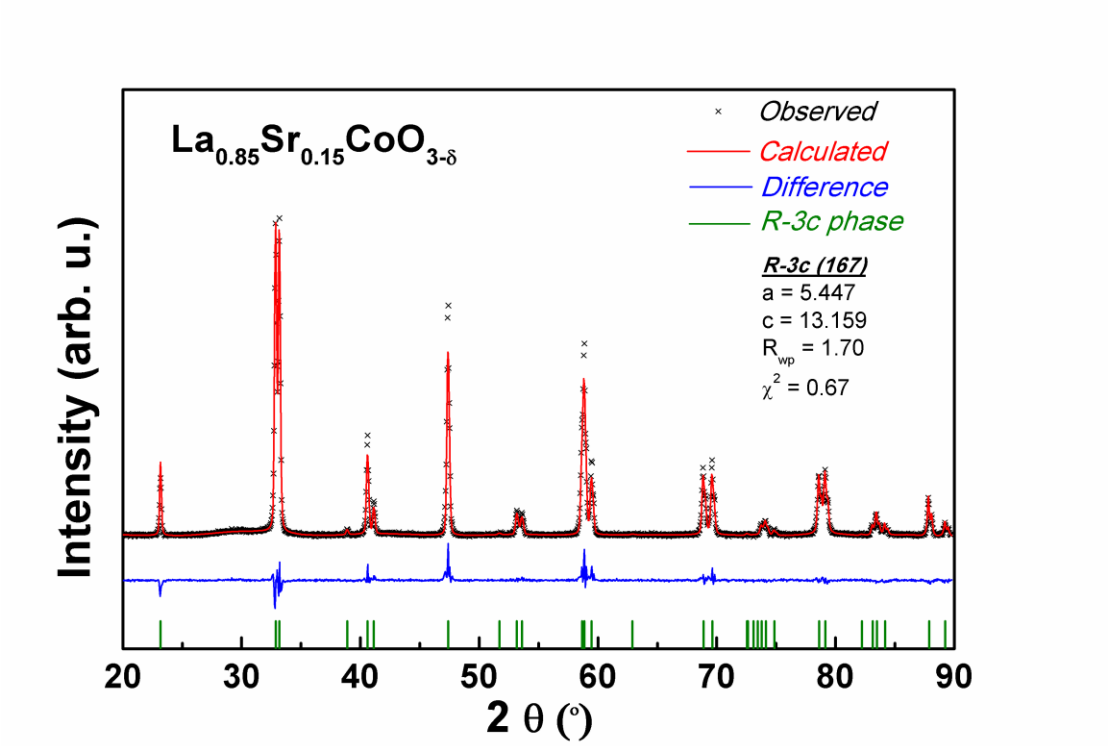

Figure 2. Powder diffractogram of $La_{0.85}Sr_{0.15}CoO_{3-\delta}$ at room temperature, together with the result of the Rietveld refinement. The compound is single phase and belongs to the hexagonal crystal system.

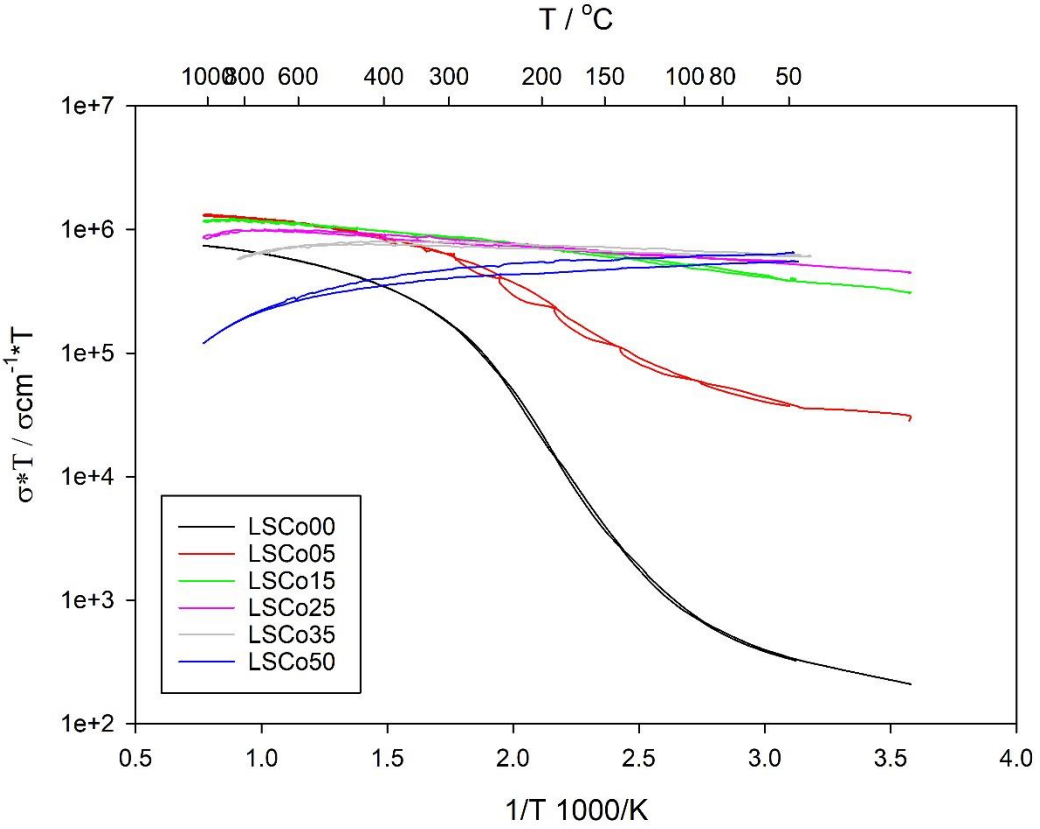

Figure 3. Total conductivities of the cobaltite's in air. The conductivity increases with temperature and in general with increasing strontium content.

The total electrical conductivity data can be found in figure 3.

The total ASR values follows a general trend (expect for at 600 ^{o}C), as the ASR values decreases with increasing strontium content. The lowest value is found for LSCo50 at 800 ^{o}C with value as low as 0.03 Ωcm^2.

All the EIS data could be fitted with two or three arcs, using two or three (RQ) in series. Q is a constant phase element with the admittance:

$$Y = Y_0(j\omega/\omega_0)^n, \quad (2)$$

where Y_0 is a constant, ω is the cyclic frequency, and n is an exponent. Y_0 and n is found from the fitting. Three representative examples are shown in figures 4-6, for LSCo00, LSCo25 and LSCo50 at 700 ^{o}C.

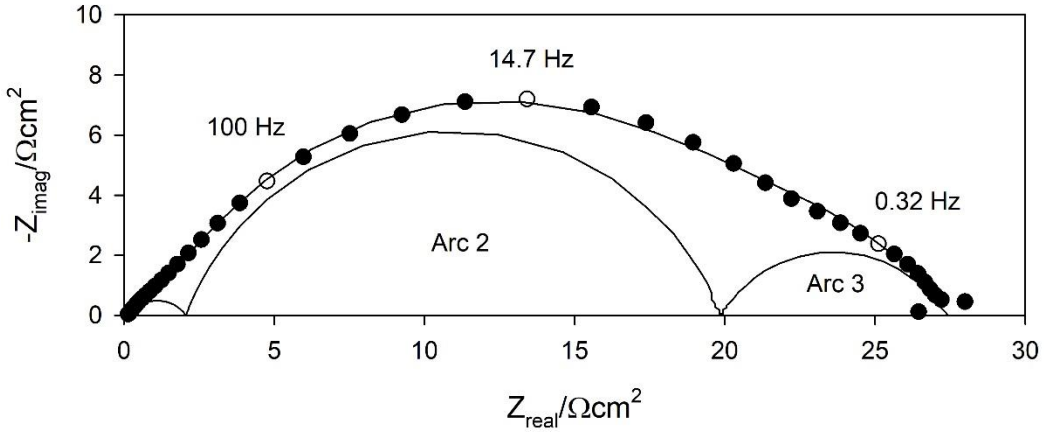

Figure 4. EIS data for LSCo00 at 700 ^{o}C in air. The fitted data is shown as a solid line. Points are measurements. The data could be de-convoluted into three arcs, as also shown in the plot.

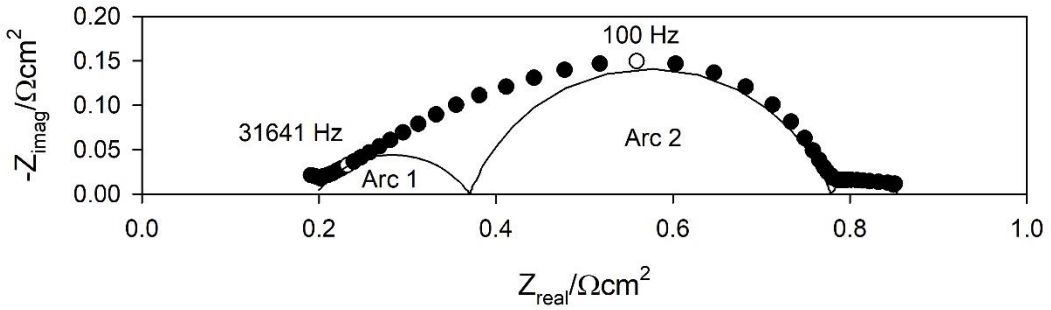

Figure 5. EIS data for LSCo25 at 700 ^{o}C in air. The fitted data is shown as a solid line. Points are measurements. The data could be de-convoluted into three arcs, as also shown in the plot.

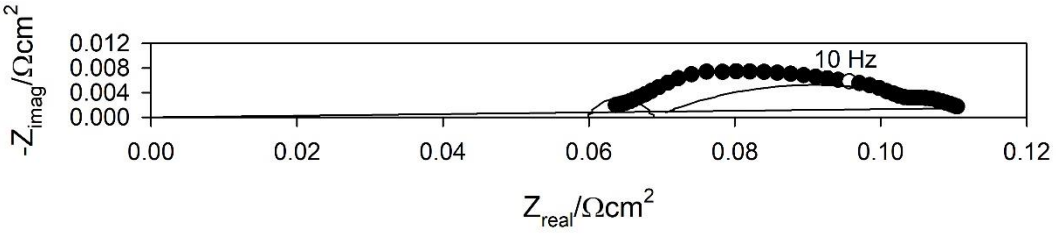

Figure 6. EIS data for LSCo50 at 700 ºC in air. The fitted data is shown as a solid line. Points are measurements. The data could be de-convoluted into two arcs, as also shown in the plot. C_{stray} has been removed for clarity.

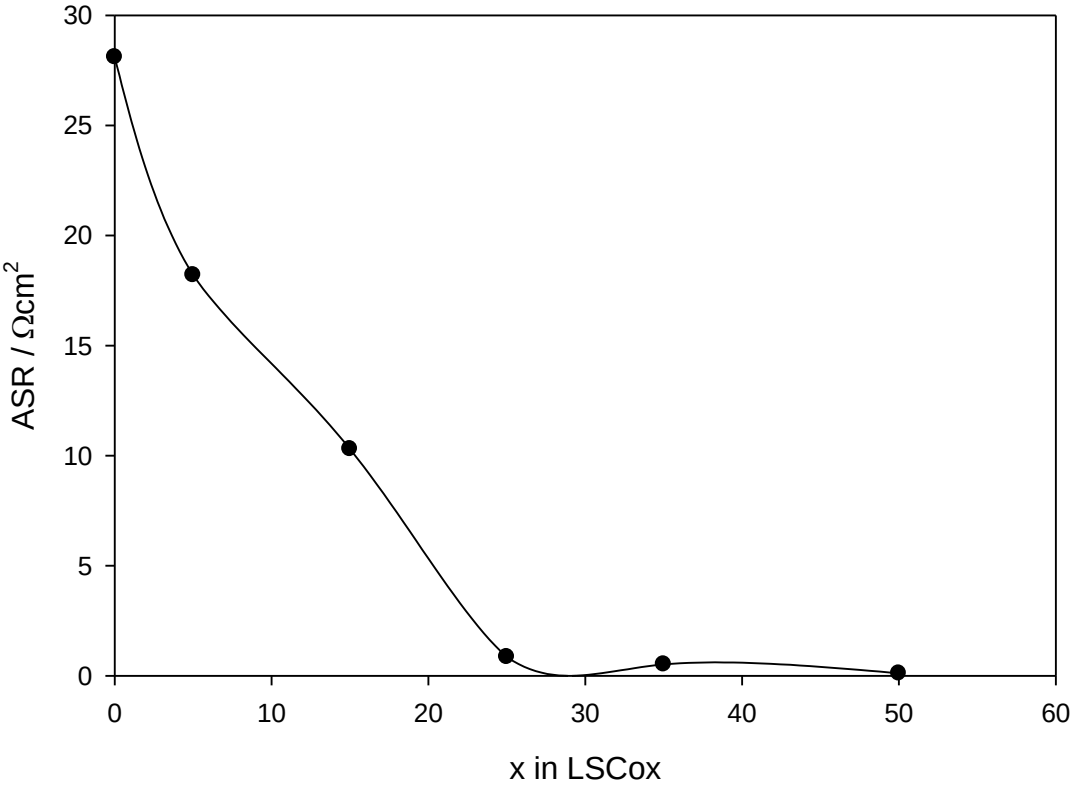

Figure 7. Total areas specific resistance of the cobaltite's in air at 700º C. The area specific resistance decreases with increasing strontium content.

As mentioned, the data are fitted with three or two arcs. The numbers in the graphs are characteristic frequencies. In figure 7 the total ASR as a function of strontium content at 700 ºC are shown. The total ASR values decreases with increasing strontium content.

The n values are the same for all the compounds at all temperatures, except for LSCo50 (the most active compound) which behaves differently from the other compounds. The individual ASR's for the two or three arcs at 700ºC can be found in Table 3, together with the n values.

Table 3. The total area specific resistance of the cobaltite's at 600, 700 and 800 ºC in air. The area specific resistance decreases with increasing temperature and strontium content. Units in Ωcm^2.

	600ºC	700ºC	800ºC
LSCo00	252	28.1	2.68
LSCo05	152	18.2	1.97
LSCo15	155	10.3	1.09
LSCo25	4.56	0.85	0.15
LSCo35	5.75	0.52	0.10
LSCo50	0.92	0.11	0.03

4. DISCUSSION

The powder XRD data agree with literature [22]. The variation of lattice parameters can be explained on the background on the Jahn-Teller effect. Co(III) is a d^6 ion which do not exhibit the Jahn-Teller effect in perovskites [23]. However, Co(IV) is a d^5 ion and can show the Jahn-Teller effect. When substituting strontium for lanthanum more Co(IV) is formed and this can explain why the a-unit cell parameter decreases and the c-unit cell parameter increases, when strontium content is increased, a clear indication of distortion of the unit cell due to the Jahn-Teller effect. The change in volume has to explained on the background of three parameters; Co(IV) formation, oxide vacancy formation and substitution of La(III) with Sr(II). Co(IV) is smaller than Co(III), oxide vacancies are smaller than oxide ions [24] and La(III) is smaller than Sr(II). When increasing the Sr(II) content, the unit cell volume first increases. This could be due to larger Sr(II) than La(III) and the formation of oxide vacancies instead of Co(IV). The difference in size between oxide ions and oxide vacancies are smaller than the difference in size between high spin Co(III) and high spin Co(IV). At larger degree of strontium substitution's, Co(IV) start to form and the unit cell volume start to decrease.

The variation in the thermal expansion coefficient with increasing strontium content can also be explained on the background of known physical parameters. At first the expansion coefficient decreases. This must due to formation of oxide vacancies, at this leads to less oxygen ions bonded per cation, leading to a higher attraction between the cation and the oxygen ion. Then the expansion coefficient starts to increase. This could be due to the formation of Co(IV), which is reduced to Co(III) at higher temperatures, leading to expansion of the perovskite oxides.

The conductivities of the cobaltite's are strongly dependent on the Sr content. Two effects are probably the reason for this. When increasing the amount of strontium more Co(IV) is formed. This leads to an increase in conductivity. However, also oxide ion vacancies are formed when doping with strontium. This leads to de-coupling of the O-Co-O super-exchange, lowering the conductivity for the high strontium substituted compounds. The conductivity behavior changes from semi-conductor like to metallic like for LSCo50.

The EIS results can be discussed in the light of a mechanism suggested in the literature for mixed ionic and electronic conductors [18]. In this mechanism the high frequency arc is due to transport of oxide ions across the electrode-electrolyte interface. The near-equivalent capacity of this arc can be calculated from equation (3) below [25]: The numbers are given in Table 4.

(3) $C_\omega = R^{(1-n)/n} Y_0^{1/n}$,

The values found at 700ºC are in the range 10^{-5} to 10^{-3} Fcm^{-2}, see Table 5, which is in fair agreement with the value expected for a double layer capacity in an electrochemical system [26]. For the high frequency arc the magnitude decreases from the strontium free cobaltite LSCo0 to the cobaltite's with a low amount of strontium. The strontium rich cobaltite has no high frequency arc.

Table 4. The area specific resistance of the individual arcs at 700 ºC in air for the cobaltite's. The medium and low frequency arcs gives the largest contributions. Units in Ωcm^2.

700ºC	R_{high}	n	R_{medium}	n	R_{low}	n
LSCo00	1.99	0.60	18.3	0.77	7.77	0.65
LSCo05	0.13	0.60	15.5	0.77	2.59	0.65
LSCo15	0.19	0.60	0.55	0.77	9.60	0.65
LSCo25	0.11	0.60	0.26	0.77	0.48	0.65
LSCo35	0.29	0.60	0.08	0.77	0.15	0.65
LSCo50	-	-	0.02	0.77	0.09	0.31

Table 5. The near equivalent capacity of the high frequency arc for the cobaltite's at 700 ºC in air is given in this table. This capacity could be due to a double layer capacity. Units in Fcm^{-2}.

X	0	5	15	25	35
C_ω	7.9e-5	9.5e-4	3.2e-5	3.9e-4	1.2e-3

The medium frequency arc can be attributed to diffusion of oxide anions through the bulk of the electrode material [18]. It is seen that the magnitude of this arc decreases with increasing strontium content. This is in good agreement with the literature, where it has been shown that the ionic conductivity increases with increasing strontium content [10].

The low frequency arc is due to a slow redox reaction at the surface of the electrode [18]. To some extent this arc is coupled with the medium frequency arc. It has been found in the literature that oxygen surface exchange reaction coupled with oxide ionic conductivity, so this is as expected. It should be noted that the n value found for LSCo50 is different from the n value found on the other cobaltites. This could indicate that a different type of elemental reaction is occurring on LSCo50 than on the other cobaltites. This compound shows metallic conductivity in the whole temperature range, in contrast to the other compounds and perhaps this could be the reason for the difference.

Another point that should be stressed is that the electro-catalytic activity of the cobaltites does apparently not depend on the oxidation state of cobalt. This could be because the valence electrons are de-localized in the cobaltite's in contrast to the i.e. the Ferrite's where the electrons are localized. In conclusion we have three cases: Manganite's where the electrons are delocalized having no ionic conductivity, Ferrite's where the electrons are localized having some ionic conductivity and the Cobaltite's where the electrons are delocalized having a relatively high ionic conductivity. The three cases behave differently. For the Manganite's a different mechanism had to be used in order to explain the results (two one-electron processes), but the behavior was like the Ferrite's, that is an intermediate compound had the highest activity, due to localized electrons on both type of compounds. For the

Ferrite's and the Cobaltite's, the same mechanism could be used to explain the results, due to the presence of oxide ionic conductivity, but the behavior was different due to localized (Fe) and delocalized electrons (Co).

The relative size of the ASR follows in the three studies follows the general trend in the literature that is the Cobaltite's has the highest activity, followed by the Ferrite's and then the Manganite's with the in general lowest activity.

5. CONCLUSION

Powder XRD shows that the cobaltite's are single phase and belongs to the hexagonal crystal system. The thermal expansion coefficient reaches is maximum for the most cobalt rich compound. The conductivity increases with increasing strontium content at temperatures below 600 ^{o}C. At higher temperatures the conductivity drops when the strontium content is higher than 15%. The activity of the cobaltite's for the reduction of the oxygen is strongly dependent on the strontium content. The strontium rich perovskite is the most active towards the reduction of oxygen. Apparently, the oxide ionic conductivity is the main factor determining the activity of the cobalt based perovskites.

ACKNOWLEDGEMENT
Dr. R. Sazinas is thanked for help with the powder XRD. Annelise Mikkelsen and Jens Østergaard's help with synthesis of the powders and preparation of bars and cones are highly appreciated.

References

1. N.Q. Minh, T. Takahashi, 'Science and technology of ceramic fuel cells', Elsevier Science B.V. (1995)
2. N.Q. Minh*, J. Am. Ceram. Soc*., 76 (1993) 563
3. Z. Zakaria, Z.A. Mat, S.H. Abu Hassan, Y.B. Kar, *Int. J. Energy Research*, 44 (2020) 594
4. M.J. Jørgensen, M.B. Mogensen, *J. Electrochem. Soc*., 148 (2001) A433-A442
5. J.M. Ralph, C. Rossignol, R. Kumar, *J. Electrochem. Soc*., 150, A1518 (2003)
6. H.Y. Tu, T. Takeda, N. Imanishi, O. Yamamoto, *Solid State Ionics*, 117 (1999) 277
7. J.F. Gao, X.Q. Liu, D.K. Peng, G.Y. Meng, *Catal. Today*, 82 (2003) 207
8. A.E. Siebert, A. Hammouche, M. Kleitz, *Electrochimica Acta*, 40 1753 (1995)
9. M.H.R. Lankhorst, H.J.M. Bouwmeester, and H. Verweij, *Physical Review Letters*, 77 (1996) 2989
10. J. Mizusaki, Y. Mima, S. Yamauchi, K. Fueki, H. Tagawa, *J. Solid State Chem*., 80 (1989) 102
11. S.B. Adler, J.A. Lane, B.C.H. Steele, *J. Electrochem. Soc*., 143 (1996) 3554
12. L.A. Chick, L.R. Pederson, G.D. Maupin, J.L. Bates, L.E. Thomas, G.J. Exarhos, *Matt. Lett*., 10 (1990) 6
13. D. N. Mueller, M. L. Machala, H. Bluhm & W. C. Chueh, *Nat. Comm*., 6 (2015) 1
14. A. Schmid, G. M. Rupp & J. Fleig, *Phys. Chem. Chem. Phys*, 20 (2018) 12016

15. P. Fabry, M Kleitz, *Electroanal. Chem. Interfac., Electrochem*., 57 (1974) 165
16. J. Newman, *J. Electrochem. Soc*., 113 (1966) 501
17. C. Xia, M. Liu, *Solid State Ionics*, 144 (2001) 249
18. K. Kammer, L. Mikkelsen, J.B. Bilde-Sørensen, *J. Solid State Electrochem*., 10 (2006) 934
19. E. Siebert, A. Hammouche, M. Kleitz, *Electrochimica Acta,* 40 (1995) 1741
20. K. Kammer Hansen, *J. Electrochem. Sci. Eng*., 8(3) (2018) 255
21. K. Kammer Hansen, *Solid State Ionics*, 344 (2020) 115096
22. B.A. Boukamp, *Solid State Ionics*, 20 (1986) 31
23. X.H. Fu, L.J. Yu, Y.T. Cui, L.Q. Xin, *J. Inorg. Organometallic Polymers Mat*., 22 (2012) 54
24. T. Schönherr, M. Atanasov, H. Adamsky, in 'Comprehensive Coordination Chemistry II', 2nd edition', 443-455 (2003), Editors-in-Chief: Jon A. McCleverty, Thomas J. Meyer
25. C. Chatzichristodoulou, P. Norby, P.V. Hendriksen, M.B. Mogensen, *J. Electroceram*. 100-107 (2015) 34
26. T. Jacobsen, B. Zachau-Christiansen, L. Bay, S. Skaarup, in Proceedings of the 17th International Symposium on Materials Science; High Temperature Electrochemistry: Ceramics and Metals, ed. F.W. Poulsen et al., Roskilde, Denmark, pp. 29 (1996)
27. N.L. Robertson, J.N. Michaels, *J. Electrochem. Soc*., 138 (1991) 1494

© 2020 The Authors. Published by ESG (www.electrochemsci.org). This article is an open access article distributed under the terms and conditions of the Creative Commons Attribution license (http://creativecommons.org/licenses/by/4.0/).